The STAM archive is now available from the IOP Publishing website http://www.iop.org/journals/STAM

ELSEVIER

Science and Technology of Advanced Materials 5 (2004) 195–200

SCIENCE AND TECHNOLOGY OF ADVANCED MATERIALS

www.elsevier.com/locate/stam

Semiconductor properties of passive films formed on sputter-deposited Fe–18Cr alloy thin films with various additive elements

Hiroaki Tsuchiya, Shinji Fujimoto*

Department of Materials Science and Processing, Graduate School of Engineering, Osaka University, 2-1 Yamada-oka, Suita, Osaka 565-0871, Japan

Received 29 August 2003; revised 26 September 2003; accepted 21 October 2003

Abstract

The semiconductor properties of passive films formed on an Fe–18Cr alloy with various additive elements in a borate buffer solution were studied using electrochemical impedance spectroscopy and photoelectrochemical response. The photocurrent was plotted as a photoelectrochemical action spectrum that could be separated into two components, which were mainly derived from Cr oxide ($E_g = 3.4$ eV) and Cr hydroxide ($E_g = 2.4$ eV). The band gap energy, E_g, of each component was almost constant, independent of the species and amount of additive elements. The photoelectrochemical response showed positive photocurrent for most potential in the passive region, which indicates that the passive film behaved as an n-type semiconductor. In addition, the Mott–Schottky plot of the capacitance showed positive slope, which also means that the passive films behaved as an n-type semiconductor. The donor density of the passive films, which can be estimated by the Mott–Schottky plots, changes depending on the film formation potentials and a variety of additives.
© 2003 Elsevier Ltd. All rights reserved.

Keywords: Passive film; Stainless steel; Additive elements; Photoelectrochemical response; Electrochemical impedance

1. Introduction

The structure and chemical composition of passive films on metals and alloys are correlated with corrosion behavior. Therefore, passive films have been subjected to ultra high vacuum (UHV) surface analysis such as Auger electron spectroscopy (AES) and X-ray photoelectron spectroscopy (XPS). On the other hand, passive films on most metals and alloys exhibit semiconductor behavior. Photoelectrochemical response and electrochemical impedance spectroscopy provide information about the semiconductor properties of passive films. For the photoelectrochemical response, the photo effect is applied into the characterization of passive films on metals and alloys. Semiconductor properties, such as band gap energy, flat band potential and type of conduction were analyzed from the current or potential change by photo irradiation. For the electrochemical impedance spectroscopy, on the other hand, the capacitance of the space charge region, which is accompanied by a bending of the electronic energy band, is measured and analyzed to estimate the donor density, flat band potential and type of conduction of passive films. The semiconductor properties of passive films on stainless steels and its constituent elements have been investigated [1–20]. The authors of the present work also examined passive films formed on pure Cr and Fe–Cr alloys in a sulfuric acid and borate buffer solution. We suggested that passive films in a sulfuric acid solution are composed of outer n-type hydroxide and inner p-type oxide layers with p–n heterojunction [21], whereas passive films in a borate buffer solution consist of an outer n-type hydroxide and an inner n-type oxide layer with isotype heterojunction [22]. Furthermore, the differences between passive films on Fe and Cr alloys formed in a sulfuric acid solution and a borate buffer solution were discussed in terms of film growth kinetics and corrosion behavior. However, the effect of additive elements on the electronic structure of passive films is still not understood.

The aim of the present study is to investigate the electronic structure of passive films formed on Fe–18Cr with additive elements, such as Ni, Co, Cu, Mo and Nb. Photoelectrochemical response and electrochemical impedance were used to obtain information on the electrochemical properties of the passive film.

* Corresponding author. Tel.: +81-6-6879-7470; fax: +81-6-6879-7471.
E-mail address: fujimoto@mat.eng.osaka-u.ac.jp (S. Fujimoto).

1468-6996/$ - see front matter © 2003 Elsevier Ltd. All rights reserved.
doi:10.1016/j.stam.2003.10.014

2. Experimental

The specimens tested were thin films of Fe–18Cr alloys with various additive elements prepared by an ion-beam sputtering technique. The deposition system has three Kaufman-type ion beam guns. Two guns were used for bombarding targets and the other was used to clean the substrate before deposition. The process chamber was evacuated to a pressure of 1.0×10^{-7} torr using a cryopump before deposition. The pressure in the chamber during deposition was 4.0×10^{-4} torr. Ar^+ions were generated by a hot electron and magnetic field, accelerated at typically 1 keV, then emitted as an Ar^+ion beam. Two Ar^+ion beams bombarded two targets simultaneously. One of the targets was Fe–18Cr sheet of 100×100 mm^2 and the other was a sheet of an additive element. The chemical composition of Fe–18Cr alloy target was as follows (at%): C: 0.025; Si: 0.30; Mn: 0.30; P: 0.003; N: 0.0064; S: 0.002; Ti: 0.30; Al: 0.17; Cr: 18.59; Ni $<$ 0.01 and Fe: bal. The substrate for deposition was a mirror-finished silicon wafer. This substrate was put on a rotating holder that is water-cooled. For cleaning, the substrate was bombarded by Ar^+ ions generated by the assist gun prior to sputtering. The deposition period was typically two hours. In the present work, Ni, Cu, Co, Mo and Nb were used as additive elements. The amount of additive element was controlled by adjusting the ion beam current on the additive element target.

A three-electrode cell consisting of a platinum counter electrode and a Ag/AgCl (3.3 M KCl) reference electrode was used. It is very difficult to remove the air-formed films in a neutral solution, as described in our previous work [22]. In this study, the specimen was activated in a dilute sulfuric acid solution and then, passivated at various potentials in the borate buffer solution. The specimen was polarized at -1000 mV$_{Ag/AgCl}$ in 0.01 mol dm^{-3} H_2SO_4 for 10 min to remove air-formed films. Finally, 0.6 mol dm^{-3} H_3BO_3 + 0.15 mol dm^{-3} $Na_2B_4O_7$ were added to the solution. The pH value of the solution was around 8.4. During the process, neither the specimen nor the solution was exposed to the atmosphere. The specimen was anodically polarized at various potentials to form a passive film. All the experiments were carried out at room temperature under continuous deaeration with high purity N_2 gas.

A monochromatic light generated using a 500 -W Xenon arc lamp with a grating monochromater was employed for the photoelectrochemical response measurements. The specimen electrode was illuminated in an electrochemical cell through a quarts window. The intensity of the exposed light was calibrated with a photo-diode optical power meter. The specimen was polarized at an applied potential for several periods to form the passive film. The photocurrent response was measured occasionally during passivation at a fixed potential. Subsequently, the applied potential was changed stepwise at intervals of 100 or 200 mV in the less noble direction. The photocurrent was also measured at each applied potential. The photoelectrochemical response was measured as the transient of current after the light was exposed and interrupted for typically 10 s. No lock-in technique was adopted.

A frequency response analyzer (FRA, NF Co., Model 5050A) equipped to the potentiostat was used for the electrochemical impedance measurements. A personal computer was used to control the FRA and to acquire and analyze the data. The imaginary part of the impedance (Z'') was measured as a function of the applied potential, and the corresponding capacitance of the space charge layer (C) was obtained from $C = -1/\omega Z''$. The capacitance of the passive film was calculated from the impedance obtained at 1 Hz, at which the Bode plot of the impedance spectra exhibits the capacitive region. The electrochemical impedance was measured occasionally in the course of the passivation at a constant potential. Then, the applied potential was changed stepwise in the less noble direction and the impedance was measured at each potential.

3. Results

3.1. Photoelectrochemical response

The photocurrent was measured for the passive films formed on Fe–18Cr in a borate buffer solution. The difference between the current just before photoirradiation and after 10 s is defined as the steady state photocurrent, i_{ph}. Since the intensity of incident light is not constant for each wavelength, the photocurrent spectra should be normalized as a photoelectrochemical action spectrum as described in the following.

Assuming that the photo excitation occurs as an indirect transition, which is usually observed in passive films on Fe, Cr, and Fe–Cr alloys, Eq. (1) describes the photocurrent spectra.

$$(i_{ph} h\nu/I_0)^{1/2} = S\cdot(h\nu - E_g), \quad (1)$$

where I_0 is the intensity and $h\nu$ the photon energy of the incident light, E_g is the band gap energy and S is a constant.

Fig. 1 shows the photocurrent spectrum plotted following Eq. (1), which is not a straight line, but exhibits a line with two regions of different slopes. As usually known, passive

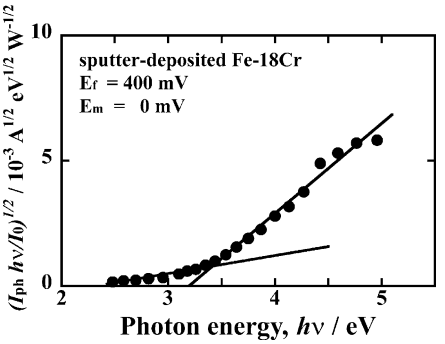

Fig. 1. Photoelectrochemical action spectra of the steady photocurrent for passive films.

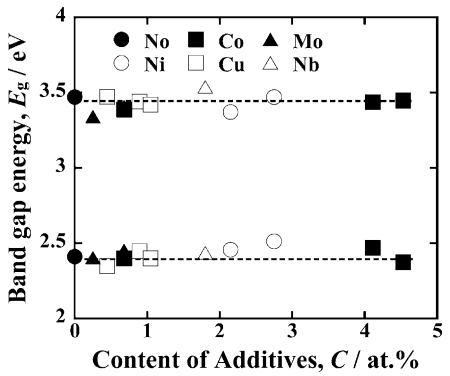

Fig. 2. Influence of various additive elements on band gap energy of passive films formed on Fe–18Cr alloy.

films consist of not single, but multi layers. Therefore, this spectrum can be separated into two components using the procedure described elsewhere [23]. E_g is estimated by the photon energy when $(i_{ph}h\nu/I_0)^{1/2}$ equals zero. Thus, E_gs were obtained as approximately 2.4 and 3.4–3.5 eV, which were nearly equivalent to that for the conventional Fe–18Cr alloy [22]. Fig. 2 shows the band gap energies of the passive films as a function of the additive element content in the substrate. The $E_g s$ are independent of the species and amount of the additive elements. Sunseri et al. [15] and the present authors [21–23] reported that E_gs of 2.4 eV and 3.4–3.5 eV are mainly derived from Cr hydroxide and Cr oxide, respectively.

Fig. 3 shows the slopes of the photocurrent spectrum, S, for passive films formed at various potentials. Positive photocurrents were generated in the hydroxide and oxide layers at most potentials, as shown in Fig. 3. The positive photo response increased as the applied potential increased. Therefore, both the hydroxide and oxide layer of passive films on Fe–18Cr alloys exhibit typical n-type

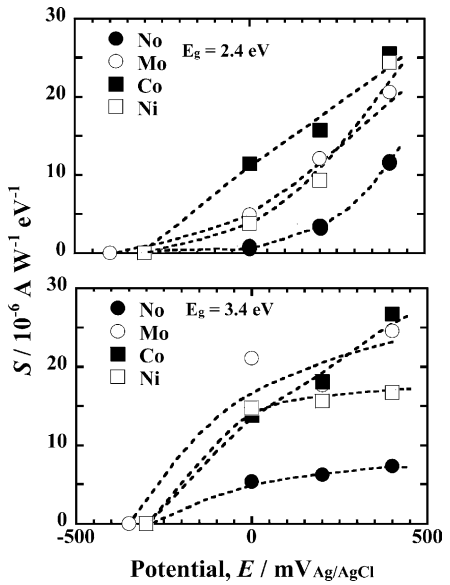

Fig. 3. Variations in the slopes of the action spectrum, S, of passive films on Fe–18Cr alloys with various additive elements.

semiconductor behavior. The observed flat band potential, E_{fb}, was approximately -300 $mV_{Ag/AgCl}$, which was also independent of additives.

Therefore, passive films on sputter-deposited Fe–18Cr exhibit the same photocurrent behavior as that of the conventional Fe–18Cr.

3.2. Capacitance of the space charge layer in passive films

The space charge region of the passive films was characterized by capacitance. Using a procedure similar to that for photocurrent measurements, the specimen was polarized at various potentials and then the applied potential was sequentially shifted in the less noble direction at intervals of 100 $mV_{Ag/AgCl}$. The capacitance was measured at each applied potential.

Assuming that the capacitance of the Helmholz layer is larger than that of the space charge region, the capacitance of a semiconductor thin film, which is polarized as the depleted state, follows the Mott–Schottky relationship (2).

$$\frac{1}{C^2} = \frac{2}{\varepsilon\varepsilon_0 qN}\left(E - E_{fb} - \frac{kT}{q}\right), \tag{2}$$

where N represents the carrier density, ε is the dielectric constant of the passive film, which is assumed as 15.6 [15,18,19], ε_0 the vacuum permittivity, q the elementary charge, k the Boltzman constant, T the absolute temperature and E_{fb} the flat band potential. In the present work, the term kT/q was ignored, as it was only about 25 mV at room temperature.

Fig. 4 exhibits the Mott–Schottky plots for the passive films formed on sputter-deposited Fe–18Cr at various applied potentials. The straight lines with positive slopes indicate typical n-type semiconductor behavior. The flat band potential, E_{fb}, is presumed to be -300 $mV_{Ag/AgCl}$, which was obtained from the intercept of the straight line to the x-axis.

Fig. 5 shows the comparison of the carrier densities in the passive films on the sputter-deposited Fe–18Cr with that on the conventional Fe–18Cr [22]. The carrier densities in the passive films on both the sputter-deposited and

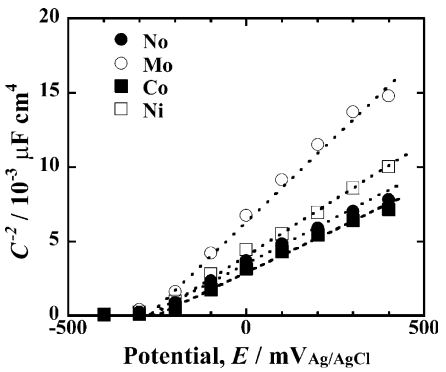

Fig. 4. Mott–Schottky plots for passive films formed on Fe–18Cr alloy with various additive elements.

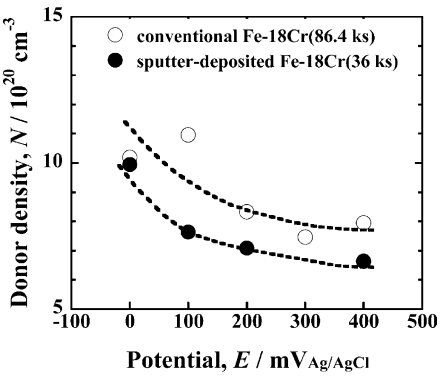

Fig. 5. Comparison of semiconductor properties of the passive films formed on sputter-deposited Fe–18Cr with that on conventional Fe–18Cr.

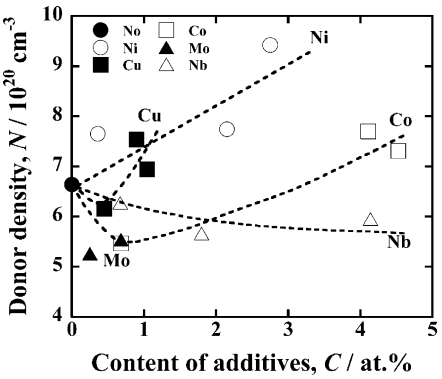

Fig. 6. Influence of additives on donor density of passive films on Fe–18Cr alloy with various additive elements.

conventional Fe–18Cr decrease as the film formation potential and the passivation time increase. The donor density for the conventional Fe–18Cr is in the range of $10^{20} - 10^{21}\,\mathrm{cm}^{-3}$, which is the same order as donor densities reported for passive films on stainless steels [15,18,19]. Furthermore, the carrier density for the sputter-deposited Fe–18Cr is smaller than that for the conventional Fe–18Cr. Fig. 6 shows the variation of carrier densities of the passive films on the sputter-deposited Fe–18Cr as a function of the additive element content in the substrate. Ni increases the carrier densities with increasing the amount of additives, whereas Cu and Co decrease these densities once in a small amount, then increase them beyond some amount of the additives. Furthermore, Nb and Mo decrease the carrier densities of the passive films formed on the sputter-deposited Fe–18Cr.

4. Discussion

4.1. Semiconductor properties of passive films on sputter-deposited Fe–18Cr

As described above, the E_gs of the passive film on the sputter-deposited Fe–18Cr thin film are almost equal to that on the conventional Fe–18Cr alloy. These results are reasonable, because the chemical compositions of the passive films formed on both materials are identical. As shown in Fig. 5, however, the carrier density for the sputter-deposited Fe–18Cr is smaller than that for the conventional Fe–18Cr. The conventional material contains minor elements such as Mn and Si, which may exist as precipitates. These precipitates should generate defects and act as a nucleation site for localized corrosion. However, precipitates contained in the sputtering target can be dissociated during the sputtering process and dissolved uniformly into the deposited film. Therefore, in the sputter-deposited film, minor elements that are usually recognized to generate defect may not be responsible for the creation of defects. Consequently, the carrier density of the passive films formed on the sputter-deposited materials should become smaller than that for conventional ones. As reported by Sugimoto et al. [24], carrier density for sputter-deposited materials is as small as that for high purity material. Furthermore, several authors have reported higher pitting corrosion resistance of sputter-deposited thin films compared with that of conventional steel with the same composition [25,26].

4.2. Electronic energy band structure model for passive films on sputter-deposited Fe–18Cr

As described in the results, the passive films formed on the sputter-deposited Fe–18Cr alloy in a borate buffer solution consists of an outer *n*-type hydroxide layer with an E_g of 2.4 eV and an inner *n*-type oxide layer with an E_g of 3.4–3.5 eV. Therefore, the two n-type semiconductor layers are simultaneously polarized at the more noble potentials than their flat band potentials to generate a depleted space charge region in each layer. Fig. 7 describes the electronic energy band model for a passive film formed on an Fe–18Cr alloy in a borate buffer solution. The proposed model has three interfaces: (I) substrate alloy/inner oxide; (II) inner oxide/outer hydroxide; and (III) outer hydroxide/electrolyte. At interface (III), the space charge region developed inside the hydroxide is in a depleted state. Therefore, the width of the depleted region increases with increasing applied

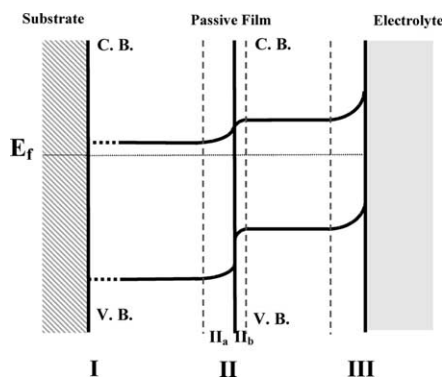

Fig. 7. A schematic presentation of the electronic band structure of passive films formed on Fe–18Cr alloy in a neutral solution.

potential, which results in a larger positive photocurrent. At interface (II), the two n-type semiconductor layers with different band gap energies are connected as an isotype heterojunction. The space charge region in the oxide layer (II_a) is also in a depleted state since the positive photocurrent is always generated and increases as the applied potential increases as shown in Fig. 3. On the other hand, the space charge region inside the hydroxide layer (II_b) may be an accumulated region because an n–n junction usually forms a depleted region in one side of the interface and an accumulated region in the other. Typically, the width of the accumulated region, which is very thin compared to that of the depleted region, is nearly constant regardless of the applied potential. Therefore, the accumulated region should not affect the photocurrent or capacitance. The electronic structure of the interface (I) is currently unknown.

4.3. Influence of additive elements on semiconductor properties of passive films

Semiconductor properties of passive film significantly influence the corrosion behavior and passive film growth of stainless steel. These properties may be affected by additive elements. Therefore, it is necessary to investigate the influence of additive elements on the semiconductor properties of passive films. However, most additive elements do not dissolve homogeneously in the alloy, but change microstructure. Therefore, it is necessary to prepare materials in which the additive elements are completely dissolved as a solid solution. As reported previously, the sputter-deposited thin film produced by the ion-beam sputtering technique consists of an equiaxed nano-crystalline without any precipitates [25,26]. Therefore, only the chemical effect of the additive elements on the semiconductor properties of the passive films can be examined.

As shown in Figs. 2 and 6, additive elements did not change the band gap energy of passive films, but did change the carrier density. The Fe substituted Cr oxide and hydroxide layers in the passive film may form some sort of three-dimensional networked structure, like the percolation model proposed by Newman and Sieradzki [27,28], for example. Additive elements might be incorporated into the passive film and substituted for Fe and/or Cr ions. Therefore, a continuously connected domain of Cr oxide and hydroxide might be formed to introduce a channel for photo-excited electrons and holes, resulting in a constant band gap energy independent of additive elements. However, incorporated additive elements should change the electronic state depending on their atomic valence. Additive elements with a higher valence than Cr(III) may decrease the defect of passive films, whereas additives with a lower valence than Cr may increase the defect. As shown in Fig. 6, therefore, Mo(VI) and Nb(VI) ions incorporated into the passive film decreased the carrier density. On the other hand, Ni(II), Cu(I or II) and Co(II) increased the carrier density. However, the influence of additive elements on the carrier density should depend on the amount of additives incorporated into the film. Therefore, small amounts of Ni and Co might decrease the carrier density.

In the present work, the role of additive elements is characterized in terms of the semiconductor properties of passive films. It is necessary to analyze the location of minute additive elements in the passive films, and evaluate the corrosion resistance in order to discuss the corrosion mechanism of stainless steel. The correlation among the electronic structure, the chemical structure and the corrosion resistance of passive films formed on Fe–18Cr alloys with various additive elements will be reported on in future studies.

5. Conclusions

The semiconductor properties of passive films formed on a sputter-deposited Fe–18Cr alloy with various additive elements in a borate buffer solution were investigated using photoelectrochemical response and electrochemical impedance spectroscopy. The photoelectrochemical response was separated into two components derived from the Cr oxide and Cr hydroxide layers. The photoelectrochemical response for each component showed a positive photocurrent in most of the passive region. Therefore, passive films on sputter-deposited Fe–18Cr with various additive elements are mainly composed of an inner n-type Cr oxide ($E_g = 3.4$ eV) and an outer *n*-type Cr hydroxide ($E_g = 2.4$ eV).

On the other hand, the Mott–Schottky plot exhibited positive slope, which suggests an n-type semiconductor property. The carrier density of the passive film, which can be estimated by the Mott–Schottky plots, changes depending on the additive elements.

Acknowledgements

This work was supported by a Grant in Aid for Scientific Research (C) sponsored by the Japan Society for the Promotion of Science, Project No. 13650778 and by The Research Foundation for Materials Science. This work was also supported by ‘Priority Assistance of the Formation of Worldwide Renowned Centers of Research—The 21st COE Program (Project:Center of Excellence for Advanced Structural and Functional Materials Designs)’ from the Ministry of Education, Sports, Culture, Science and Technology of Japan.

References

[1] S.M. Wilhelm, N. Hackerman, Photoelectrochemical characterization of the passive films on iron and nickel, J. Electrochem. Soc. 128 (1981) 1668–1674.

[2] U. Stimming, Properties of the passive film on iron electrodes by capacity and photocurrent measurement, in: M. Froment (Ed.), Proc. Int. Conf. Passivity Metals Semiconductors, 1983, pp. 477–482.
[3] R.C. Searson, R.M. Latanision, U. Stimming, Analysis of the photoelectrochemical response of the passive film on iron in neutral solution, J. Electrochem. Soc. 135 (1988) 1358–1383.
[4] L.M. Peter, J. Li, R. Peat, Surface recombination at semiconductor electrodes, J. Electroanal. Chem. 165 (1984) 29–40.
[5] K. Azumi, T. Ohtsuka, N. Sato, Analysis of transient photocurrent in passivated iron electrode in neutral borate solution, J. Jpn Inst. Metals 53 (1989) 479–486.
[6] K. Azumi, T. Ohtsuka, N. Sato, An analysis of transient photocurrents measured on passivated iron electrode, Corros. Sci. 31 (1990) 715–720.
[7] H. Gerischer, Remarks on the electronic structure on the oxide film on passive iron and the consequences for its electrode behaviour, Corros. Sci. 29 (1989) 191–195.
[8] H. Gerischer, Models for the discussion of the photo-electrochemical response of oxide layers on metals, Corros. Sci. 29 (1989) 257–266.
[9] H. Gerischer, On the interpretation of photoelectrochemical experiments with passive layers on metals, Corros. Sci. 31 (1990) 81–88.
[10] H. Gerischer, The impact of semiconductors on the concepts of electrochemistry, Electrochim. Acta 35 (1990) 1677–1699.
[11] F. Di Quarto, S. Piazza, C. Sunseri, A photocurrent spectropic investigation of passive films on chromium, Corros. Sci. 31 (1990) 721–726.
[12] E.-A. Cho, H.-S. Kwon, D.D. Macdonald, Photoelectrochemical analysis of the passive film formed on Fe–20Cr in pH 8.5 buffer solution, Electrochim. Acta 47 (2002) 1661–1668.
[13] J.-S. Kim, E.-A. Cho, H.-S. Kwon, Photo-electrochemical analysis of passive film formed on Cr in pH 8.5 buffer solution, Electrochim. Acta 47 (2001) 415–421.
[14] A. Di Paola, Study of passive films on stainless steels by photocurrent measurements, Corros. Sci. 31 (1990) 739–744.
[15] C. Sunseri, S. Piazza, F. Di Quarto, Photocurrent spectroscopic investigations of passive films on chromium, J. Electrochem. Soc. 137 (1990) 2411–2417.
[16] A.M.P. Simões, M.G.S. Ferreira, B. Rondot, M. da C Belo, Study of passive films formed on AISI 304 stainless steel by impedance measurements and photoelectrochemistry, J. Electrochem. Soc. 137 (1990) 82–87.
[17] P. Schmuki, H. Böhni, Semiconductive properties of passive films and susceptibility to localized corrosion, Werkst Korros 42 (1991) 203–207.
[18] P. Schmuki, H. Böhni, Metastable pitting and semiconductive properties of passive films, J. Electrochem. Soc. 139 (1992) 1908–1913.
[19] R. Babić, M. MetikoŠ-Huković, Semiconducting properties of passive films on AISI 304 and 316 stainless steels, J. Electroanal. Chem. 358 (1993) 143–160.
[20] A. Di Paola, Semiconducting properties of passive films on stainless steels, Electrochim. Acta 34 (1989) 203–210.
[21] H. Tsuchiya, S. Fujimoto, O. Chihara, T. Shibata, Semiconductive behavior of passive films formed on pure Cr and Fe–Cr alloys in sulfuric acid solution, Electrochim. Acta 47 (2002) 4357–4366.
[22] H. Tsuchiya, S. Fujimoto, T. Shibata, submitted for publication.
[23] S. Fujimoto, O. Chihara, T. Shibata, Photo electrochemical response of passive films formed on pure Cr and Fe–Cr alloys in sulphuric acid solution, Mater. Sci. Forum 289–292 (1998) 989–996.
[24] K. Sugimoto, S. Matsuda, M. Isshiki, T. Ejima, K. Igaki, Corrosion characteristics of high purity iron, J. Jpn Inst. Metals 46 (1982) 155–161.
[25] S. Fujimoto, H. Umemura, M. Kurihara, H. Tsuchiya, T. Shibata, Effect of additive elements on electrochemical behaviour of passive films on Fe–18Cr alloy, Corros. Sci. Tech. 31 (2002) 29–33.
[26] S. Fujimoto, H. Hayashida, T. Shibata, Extremely high corrosion resistance of thin film stainless steels deposited by ion beam sputtering, Mater. Sci. Engng A267 (1999) 314–318.
[27] K. Sieradzki, R.C. Newman, A percolation model for passivation in stainless steels, J. Electrochem. Soc. 133 (1986) 1979–1980.
[28] S. Qian, R.C. Newman, R.A. Cottis, K. Sieradzki, Validation of a percolation model for passivation of Fe–Cr alloys: two-dimensional computer simulations, J. Electrochem. Soc. 137 (1990) 435–439.